High power pulsed fiber MOPA system incorporating electro-optic modulator based adaptive pulse shaping

Andrew Malinowski, Khu Tri Vu, Kang Kang Chen, Johan Nilsson, Yoonchan Jeong, Shaiful Alam, Dejiao Lin and David J. Richardson*

Optoelectronics Research Centre, University of Southampton, Southampton, SO17 1BJ, UK
**djr@orc.soton.ac.uk*

Abstract: We demonstrate active pulse shaping using an Electro-Optic Modulator in order to compensate the pulse shaping effects caused by Gain Saturation in a high power Yb doped fiber amplifier chain and to generate various custom-defined output pulse shapes. Square, step and smooth pulse shapes are achieved, with mJ pulse energies. Use of a modulator to shape pulses rather than direct modulation of the diode drive current allows us to eliminate undesired transients due to laser start up dynamics. The required shaping is calculated based on a simple measurement of amplifier performance, and does not require detailed modeling of the amplifier dynamics.

OCIS codes: (060.2320) Fiber optics amplifiers and oscillators; (140.2020) Diode lasers.

References and links

1. B. Desthieux, R. I. Laming, and D. N. Payne, "111 kW (0.5 mJ) pulse amplification at 1.5 μm using a gated cascade of three erbium-doped fiber amplifiers," Appl. Phys. Lett. **63**(5), 586–588 (1993).
2. D. Taverner, D. J. Richardson, L. Dong, J. E. Caplen, K. Williams, and R. V. Penty, "158-microJ pulses from a single-transverse-mode, large-mode-area erbium-doped fiber amplifier," Opt. Lett. **22**(6), 378–380 (1997).
3. S. A. Guskov, S. V. Popov, S. Chernikov, and J. R. Taylor, "Second harmonic generation around 0.53 μm of seeded Yb fibre system in periodically-poled lithium niobate," Electron. Lett. **34**(14), 1419–1420 (1998).
4. P. Dupriez, A. Piper, A. Malinowski, J. K. Sahu, M. Ibsen, B. C. Thomsen, Y. Jeong, L. M. B. Hickey, M. N. Zervas, J. Nilsson, and D. J. Richardson, "High average power, high repetition rate, picosecond pulsed fiber master oscillator power amplifier source seeded by a gain-switched laser diode at 1060 nm," IEEE Photon. Technol. Lett. **18**(9), 1013–1015 (2006).
5. P. Dupriez, C. Finot, A. Malinowski, J. K. Sahu, J. Nilsson, D. J. Richardson, K. G. Wilcox, H. D. Foreman, and A. C. Tropper, "High-power, high repetition rate picosecond and femtosecond sources based on Yb-doped fiber amplification of VECSELs," Opt. Express **14**(21), 9611–9616 (2006).
6. R. Paschotta, J. Nilsson, A. C. Tropper, and D. C. Hanna, "Ytterbium-Doped Fiber Amplifiers," IEEE J. Quantum Electron. **33**(7), 1049–1056 (1997).
7. L. M. Frantz, and J. S. Nodvik, "Theory of Pulse Propagation in a Laser amplifier," J. Appl. Phys. **34**(8), 2346–2349 (1963).
8. Y. Wang, and H. Po, "Dynamic Characteristics of Double-Clad Fiber Amplifiers for High-Power Pulse Amplification," J. Lightwave Technol. **21**(10), 2262–2270 (2003).
9. W. Williams, C. Orth, R. Sacks, J. Lawson, K. Jancaitis, J. Trenholme, S. Haney, J. Auerbach, M. Henesian, and P. Renard, "NIF Design Optimization," in *Inertial Confinement Fusion Annual Report*, (Lawrence Livermore National Laboratory, 1996) p. 184.
10. M. Shaw, W. Williams, R. House, and C. Haynam, "Laser Performance Operations Model (LPOM)," in *Inertial Confinement Fusion Semiannual Report* (Lawrence Livermore National Laboratory, 2004).
11. W. Shaikh, I. O. Musgrave, A. S. Bhamra, and C. Hernandez-Gomez, "Development of an amplified variable shaped long pulse system for Vulcan," in *Central Laser Facility Annual Report* (CCLRC Rutherford Appleton Laboratory, 2005/2006) p. 199.
12. K. T. Vu, A. Malinowski, D. J. Richardson, F. Ghiringhelli, L. M. B. Hickey, and M. N. Zervas, "Adaptive pulse shape control in a diode-seeded nanosecond fiber MOPA system," Opt. Express **14**(23), 10996–11001 (2006).
13. D. N. Schimpf, C. Ruchert, D. Nodop, J. Limpert, A. Tünnermann, and F. Salin, "Compensation of pulse-distortion in saturated laser amplifiers," Opt. Express **16**(22), 17637–17646 (2008).
14. A. E. Siegman, *Lasers*, (University Science Books, Sausalito, CA, 1986).
15. E. Lichtman, A. A. Friesem, R. G. Waarts, and H. H. Yaffe, "Stimulated Brillouin-Scattering Excited By 2 Pump Waves In Single-Mode Fibers," J. Opt. Soc. Am. B **4**(9), 1397–1403 (1987).

#117239 - $15.00 USD Received 14 Sep 2009; accepted 15 Oct 2009; published 2 Nov 2009

16. R. G. Smith, "Optical Power Handling Capacity of Low Loss Optical Fibers as Determined by Stimulated Raman and Brillouin Scattering," Appl. Opt. **11**(11), 2489 (1972).
17. J. W. Dawson, M. J. Messerly, R. J. Beach, M. Y. Shverdin, E. A. Stappaerts, A. K. Sridharan, P. H. Pax, J. E. Heebner, C. W. Siders, and C. P. Barty, "Analysis of the scalability of diffraction-limited fiber lasers and amplifiers to high average power," Opt. Express **16**(17), 13240–13266 (2008).
18. C. Jauregui, J. Limpert, and A. Tünnermann, "Derivation of Raman treshold formulas for CW double-clad fiber amplifiers," Opt. Express **17**(10), 8476–8490 (2009).
19. S. Kirkpatrick, C. D. Gelatt, Jr., and M. P. Vecchi, "Optimization by Simulated Annealing," Science **220**(4598), 671–680 (1983).

1. Introduction

At present, bulk solid state Q-switched lasers based on Nd:YAG operating at 1064 nm represent the workhorse technology used for industrial materials processing in the nanosecond regime. However, with pulse energies now entering the multi-mJ regime, fiber based technology is increasingly beginning to compete in the market place within a number of these application areas. Fiber based systems offer a number of attractive features for industrial applications including alignment-free operation, compact cavity designs, high wall-plug efficiencies, high reliability and exceptional beam quality. A further highly significant feature is the flexibility in the output radiation format in terms of pulse duration, repetition-rate and peak powers. This flexibility is perhaps best exemplified by diode-seeded fiber based Master Oscillator Power Amplifier (MOPA) systems which have been shown to be capable of high peak and average power operation in the femtosecond, picosecond through to the nanosecond and longer pulsed regimes by appropriate choice of seed laser technology and associated electrical/optical drive conditions [1–5].

Further flexibility can potentially be achieved by the ability to temporally shape the laser pulses. For example, the prospect of generating rectangular pulses of uniform intensity offers obvious advantages for frequency conversion applications, or it can be used to maximize the pulse energy from the fiber MOPA itself by keeping the instantaneous power just below the Raman threshold for the duration of the pulse (ordinarily Raman scattering (SRS) acts as a cap on peak power at the signal wavelength, by efficiently scattering the light to other wavelengths). Similarly, multi-level pulses offer potential benefits in material processing applications where for example an initial high intensity pulse component might be used to initiate a process and subsequently a lower power level might be used to sustain and control it.

Pulse shape evolution is significant in mJ fiber MOPA systems due to the relatively modest saturation energies associated with the confined optical mode within the fiber [6], which results in significant pulse reshaping over the timescale of the pulse within the amplifier chain due to depletion of the population inversion. Assuming a square input pulse, this reshaping effect causes the pulse to have a very high peak power at its leading edge and to exponentially decrease towards the trailing edge [7,8].

It is possible to achieve control of the output pulse shape by actively controlling the shape of the input pulse so as to pre-compensate for the effects of the gain saturation. This has been demonstrated experimentally using feed-back loops to optimize the pulses [9–12], or by simulating the amplifier performance and calculating the required pulse analytically [13].

We previously demonstrated a fiber MOPA operating at mJ pulse energies which incorporated an adaptive algorithm designed to modulate the semiconductor diode seed laser current in such a way as to generate user defined pulses at the system output [12]. In this demonstration the power levels were relatively modest (~10 W average power), and the quality and range of pulse shapes that could be generated were compromised to an extent by the frequency response of the diode drive electronics, and the limited dynamic range (~10 dB) that could be reliably achieved in terms of diode seed power control. As we pointed out in this earlier work, using an Electro-Optic Modulator (EOM), which can have a bandwidth of tens of Gigahertz and high extinction ratio, offers the potential for much better performance (albeit at increased cost).

In this paper we demonstrate an EOM based shaping technique for use within a MOPA system and report an actively shaped MOPA system operating at far higher powers (>200 W) than previously demonstrated. Using active pulse shaping at the amplifier input we show that

#117239 - $15.00 USD Received 14 Sep 2009; accepted 15 Oct 2009; published 2 Nov 2009

it is possible to generate a range of customer defined pulse shapes at the final output in a very straightforward fashion. We note that simulation or detailed investigation of the amplifier performance is unnecessary: a single measurement of the propagation of an arbitrary test pulse and a simple fitting process providing sufficient information to generate any other pulse shape with reasonable quality. This allows the technique to be adapted in short order to any amplifier chain.

As examples we demonstrate the generation of high energy square optical pulses, as well as the generation of both two-step pulses and smooth pulses of various shapes.

2. Theory of pulse shaping

If we assume steady state pumping and that the duration of pulses is short compared to the pulse period, and short compared to the excited state lifetime (of order 1 ms), it is reasonable to assume that the additional build up of the excited state due to the pump during the duration of the pulse is negligible, and that the amount of ASE is very small. The emission cross-section of an Yb doped silica fiber at wavelengths around 1060 nm is much larger than the absorption cross section. Therefore, during the time the pulse travels through the laser medium, only the emission cross-section at the signal wavelength needs to be taken into account.

Given these assumptions, and a homogeneous gain medium, the intensity in an amplifier is governed by the following pair of rate Eqs. (14):

$$\frac{\partial \hat{I}(\hat{z},\hat{t})}{\partial \hat{t}} + c\frac{\partial \hat{I}(\hat{z},\hat{t})}{\partial \hat{z}} = \sigma c \hat{N}(\hat{z},\hat{t})\hat{I}(\hat{z},\hat{t}) \tag{1}$$

$$\frac{\partial}{\partial \hat{t}}\Delta\hat{N}(\hat{z},\hat{t}) = -\left(\frac{2^*\sigma}{\hbar\omega}\right)\hat{N}(\hat{z},\hat{t})\hat{I}(\hat{z},\hat{t}) \tag{2}$$

where σ is the cross-section for stimulated emission, N is the inversion, and 2* is the "saturation factor", which varies between 1 and 2 depending on how quickly the lower laser level empties. Applying a transform ($z \equiv \hat{z}, t \equiv \hat{t} - \hat{z}/c$) to convert to a coordinate system which moves with the forward travelling pulse converts these equations to the form:

$$\frac{\partial I(z,t)}{\partial z} = \sigma N(z,t) I(z,t) \tag{3}$$

$$\frac{\partial N(z,t)}{\partial \hat{t}} = -\left(\frac{2^*\sigma}{\hbar\omega}\right)N(z,t)I(z,t) \tag{4}$$

These equations can be rearranged and integrated to the form

$$I_{out}(t) = I_{in}(t)e^{\sigma N_{tot}(t)} = G(t)I_{in}(t) \tag{5}$$

$$\frac{dN_{tot}(t)}{dt} = \frac{2^*}{\hbar\omega}[I_{out}(t) - I_{in}(t)] \tag{6}$$

where

$$N_{tot}(t) \equiv \int_{z=0}^{z=L} N(z,t)dz \text{ and } G(t) \equiv e^{\sigma N_{tot}(t)} \tag{7}$$

If we adopt the following definitions; $N_0 \equiv \int_{z=0}^{z=L} \hat{N}(\hat{z},\hat{t}_0)d\hat{z}$ - the total initial inversion; $G_0 \equiv e^{\sigma N_0}$ - the initial amplifier gain; $U_{in}(t) \equiv \int_{t_0}^{t} I_{in}(t)dt$ and $U_{out}(t) \equiv \int_{t_0}^{t} I_{out}(t)dt$ - the input

#117239 - $15.00 USD Received 14 Sep 2009; accepted 15 Oct 2009; published 2 Nov 2009

and output pulse energies per unit area from starting time until time t, and $U_{sat} \equiv \frac{\hbar\omega}{2^*\sigma}$ - the saturation energy per unit area, these equations have an analytical solution of the form [14]:

$$I_{out}(t) = I_{in}(t)G(t) \tag{8}$$

where the gain $G(t)$ is given by:

$$G(t) = 1 + (G_0 - 1)e^{-U_{out}(t)/U_{sat}} \tag{9}$$

or equivalently

$$G(t) = 1 + (G_0 - 1)e^{-E_{out}(t)/E_{sat}} \tag{10}$$

where $E_{out}(t) = U_{out}(t)A_{eff}$, $E_{sat} = U_{sat}A_{eff}$.

This expression can be inverted in order to establish the input $I_{in}(t)$ required to obtain the desired output $I_{out}(t)$ as a function of the small signal gain G_0, $E_{out}(t)$, and E_{sat}, i.e.

$$I_{in}(t) = \frac{I_{out}(t)}{1 + (G_0 - 1)e^{-E_{out}(t)/E_{sat}}} \tag{11}$$

At this point, in order to calculate pulse evolution we need only know G_0 and E_{sat}. Thus, if we can obtain G_0 and E_{sat} experimentally for a given amplifier at a given pump power, we can use the above equation to calculate the required input pulse shape required to obtain a desired output pulse shape without any detailed knowledge of the fundamental amplifier characteristics, such as the cross-section, effective area, length, or inversion distribution.

3. MOPA setup

Our MOPA comprises a diode laser and three amplifier stages. A schematic of the setup is shown in Fig. 1. The seed is a commercially packaged, fiber-pigtailed diode laser operating at a wavelength of 1061nm (with a free-running bandwidth ~3 nm). The diode generates pulses with an output peak power of ~700mW. The broad spectrum is actually composed of several very narrow lines spaced by ~0.2 nm, the mode spacing determined by the length of the diode cavity. A fiber Bragg grating (FBG) is spliced to the diode output at a distance of ~2m from the fiber facet. By attaching a grating, which has a larger reflectivity (~5%) than the diode front facet, we create a longer cavity with a bandwidth set by the grating reflectivity characteristics and very many cavity modes within the envelope, creating a smooth spectrum with 0.3 nm width. This yields of order 600 cavity modes (mode separation ~100 MHz) compared to the diode spectrum without the FBG which consists of only a small number of longitudinal modes (~25), and as a result would be expected to be subject to stimulated Brillouin scattering (SBS) in the fiber amplifiers at the power levels encountered in this work. Since the SBS bandwidth in our silica fibers is ~50 MHz for a wavelength of 1061 nm, the individual cavity modes would be expected to generate SBS effectively independently, and the effective SBS threshold will be approximately proportional to the number of modes [15]. Indeed, we observed no evidence of SBS during our experiments with this line-narrowed laser.

#117239 - $15.00 USD Received 14 Sep 2009; accepted 15 Oct 2009; published 2 Nov 2009

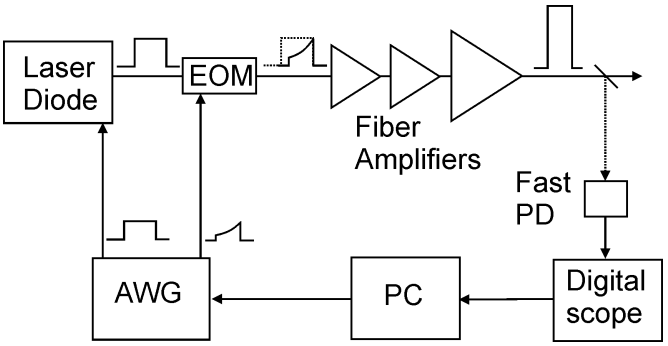

Fig. 1. Schematic of active pulse shaping system with EOM

The diode was mounted in a commercial drive board which allowed its drive current to be controlled at repetition rates of up to several 100 kHz using one channel of a computer controlled Arbitrary Waveform Generator (AWG). The pulse duration set on this pulse generator could be changed from tens of nanoseconds to tens of microseconds as desired. In general the AWG provided a square pulse with a duration slightly longer than that of the pulse ultimately targeted. Operating the diode in pulsed mode allowed us to utilize larger diode peak powers (up to the full 700 mW) whilst keeping the average power below the 50 mW operating limit of our EOM.

The output from the diode was fed through the EOM, which has a 20 GHz response with 30 dB extinction ratio, and which was synchronously driven from the second channel of the AWG. The EOM was used to carve the required amplifier input pulse forms from the square pulse output from the diode. The first 100ns of the pulse from the seed laser was eliminated in the carving process, since the diode had a rise time of tens of nanoseconds and it takes several tens of nanoseconds to stabilize the amplitude. Moreover, this represents several round trip times of the external cavity defined by the FBG, so that we can be confident that after this time the diode is emitting with the desired, SBS-safe, densely mode-spaced spectrum.

The AWG has 16-bit amplitude resolution and a time resolution of 4 ns. The optical power transmission of the EOM varies sinusoidally rather than linearly with applied voltage. This is taken into account when calculating the control voltage waveform which is sent to the EOM in order to ensure that the desired output optical pulse form is obtained in the carving process. An isolator was spliced between the seed laser and the amplifier chain. Due to losses in the EOM and isolator totaling ~6 dB, the peak seed power to the amplifier system is ~175 mW.

The amplifier system comprises three distinct diode-pumped Yb-doped amplifier stages. The first two stages are fully fiberised. A core-pumping scheme incorporating a 4 m length of ytterbium doped single mode fiber is used for the first stage and a 8 m length cladding pumped fiber amplifier with a 10 μm core diameter and 0.07 NA (mode field diameter (MFD)~11μm) for the second stage. The single mode pump radiation (300mW at 976nm) was coupled into the first stage by a 976nm/1060nm WDM coupler. The multimode pump radiation (7W at 915nm) was delivered into the second stage amplifier by a tapered fiber bundle (TFB). The amplifier fibers in both stages are approximately single mode and the output at the second stage has an M^2<1.2. The maximum saturated average output powers from the two amplifiers were 50 mW and 3 W from stages 1 and 2, respectively. Typically, small signal gains were up to 20 dB in the first stage (depending on duty cycle) and about 20 dB in the second stage, with losses of the order of 2 dB between stages, due to the isolator.

The final (third) amplifier stage was end-pumped using a 500 W 975 nm diode stack. The pump power of this stage was varied during the experiments, while the first two stages were operated with fixed pump powers. The final stage amplifier fiber has a 30μm core diameter and 0.06 NA (MFD~24μm) and 400μm diameter cladding, was 10 m long and was typically operated with a gain around or below 20dB. The core was theoretically multimode (supporting ~5 modes), but with appropriate signal launch, the amplified output was close to

#117239 - $15.00 USD Received 14 Sep 2009; accepted 15 Oct 2009; published 2 Nov 2009

single-mode (M^2~1.5). The peak gain through the whole amplifier chain (including losses due to isolation) was up to ~55 dB. The highest output peak power that we measured was about 35kW. The Stimulated Raman Scattering (SRS) threshold for this amplifier was estimated [16–18] at 80 kW, well above any instantaneous power obtained in the experiments described, and the estimated SBS threshold was well over 100 kW.

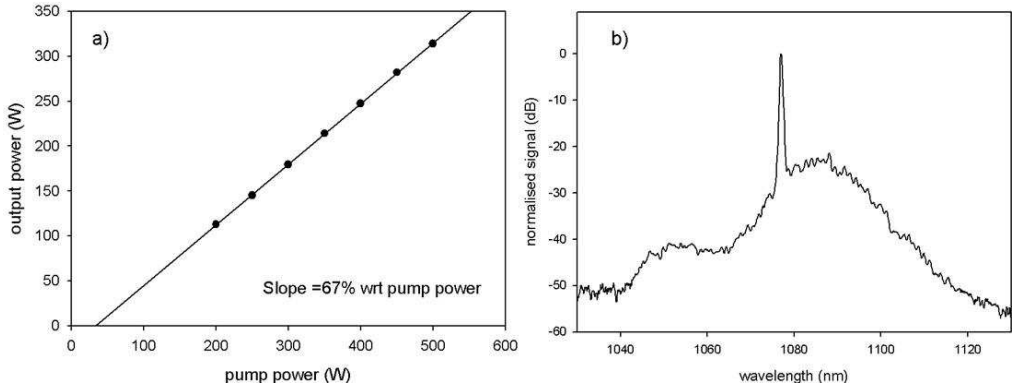

Fig. 2. (a) MOPA output power curve and (b) output spectrum (resolution 0.5 nm) at 200W and 1% duty cycle

Figure 2 shows the average output power of the MOPA plotted against the output of the pump laser of the final stage. The amplifier slope efficiency was 67% with respect to the launched pump power. The spectrum did not broaden significantly compared to the initial bandwidth of 0.3 nm during amplification. These measurements were taken using 100 ns pulses and a 1% duty cycle.

4. Pulse shaping method

To determine the parameters for the pulse shaping, we make a measurement of the output of the MOPA for a test input pulse at a particular power level. Any pulse shape or duration can be chosen for the input pulse; however a square pulse of the same duration as the target pulse was typically used for convenience. The pulses are sampled and detected by a 1 GHz photodiode which is connected to a 500 MHz oscilloscope under computer control. By comparing the input and output pulses we obtain a measurement of the instantaneous gain G(t) at each point in the pulse. By iteratively fitting this data to Eq. (10), numerically integrating to obtain $E_{out}(t)$, we obtain an estimate of E_{sat} and G_0. The fitting process takes just a few seconds. We then directly calculate the required input pulse from our chosen output pulse shape utilizing Eq. (11) and our measured values of E_{sat} and G_0 (again using numerical integration to give $E_{out}(t)$). We make no assumptions about the details of the gain distribution within the system, so, unlike [13], we require no simulation or detailed knowledge of the amplifier chain.

In our previous work [12], we used an iterative approach based on the simulated annealing (SA) method [19], where the input pulse is defined by a few parameters which can be varied, with the effects on the output pulse being monitored. We experimentally compared this approach with the direct calculation approach described above. As a first stage, in order to reduce experimental time in this work, we simulated the output pulse shapes based on Eq. (7) and our measured values of E_{sat} and G_0, rather than using the experimental shaping results. As a second stage of optimization, we used the outcome of the first optimization stage as the initial seed pulse to the MOPA. In this way, we start our experimental iterative process with what we hope is a close approximation to the final solution and this greatly reduces the required experimental time to obtain the output pulse form. We then measure the resulting output pulse and use the SA method to further iteratively improve the output pulse based on the real amplifier performance, exactly as we did in our previous work. We would expect that,

#117239 - $15.00 USD Received 14 Sep 2009; accepted 15 Oct 2009; published 2 Nov 2009

if we have chosen our optimization parameters for the iterative method well, we will obtain the same choice of input pulse shape from the direct calculation method and performing the iterative method in simulation, since both are based on our model of amplifier performance. However, we might expect the iterative solution based on experimental results to perform better, because it attempts to optimize against real outputs of the amplifier, rather than calculated outputs.

5. Pulse shaping results

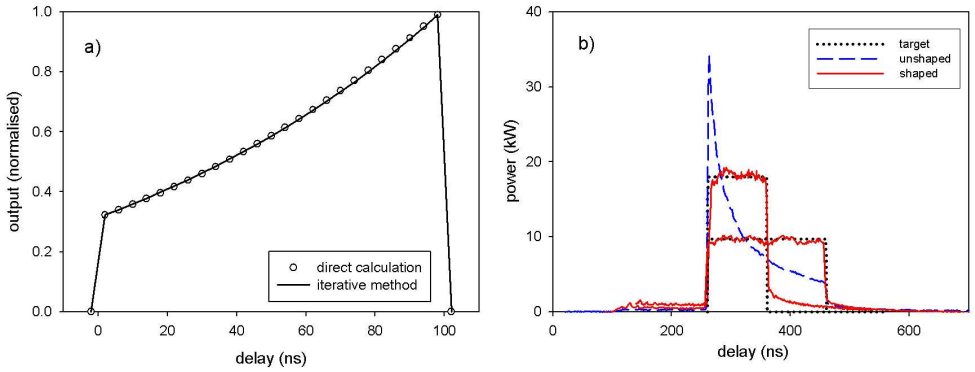

Fig. 3. (a) Input pulses to generate a square 100ns output pulse, produced by direct calculation or iterative method, (b) Square output pulses with 100 and 200 ns pulse durations.

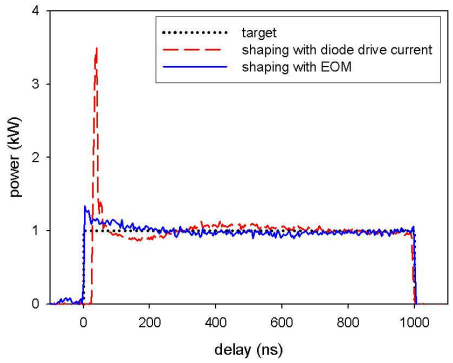

Fig. 4. Square pulses generated via modulating diode current or modulating EOM

Figure 3(a) shows the optimized input pulse shapes for a targeted 100ns pulse produced by the iterative approach using simulated amplifier response (using an exponentially ramped input pulse specified by the height of the starting point of the ramp, an exponential factor and a fixed pulse width, as described in [12]) and by the direct calculation method. Data points are spaced by 4 ns to match the resolution of the AWG. Direct calculation of the required input pulses based on Eq. (11) produced pulses which were virtually indistinguishable from those obtained using the iterative method in simulation (less than 1% deviation in amplitude across the entire pulse shape between the two methods for all pulse durations considered). Typically of order 20 iterations were required to achieve convergence.

Figure 3(b) shows various pulses produced at a pump power level of 350W, corresponding to an average MOPA output power of 200W. The pulse repetition rate was 100 kHz and the pulse energy was 2 mJ. The long-dashed curve is the shape of the output pulse from the amplifier when the seed pulse was a 200ns duration square pulse. Based on fitting this pulse

#117239 - $15.00 USD Received 14 Sep 2009; accepted 15 Oct 2009; published 2 Nov 2009

we obtained a saturation energy for our amplifier of 0.6 mJ, so we are operating ~3-4 times above saturation energy. It can be seen that reshaping is significant, with the leading edge of the pulse having an instantaneous power of 35 kW, which has dropped to ~4 kW after 200 ns. The FWHM width of this pulse is only about 20 ns.

It should be noted that, based on the effective areas of the various amplifier fibers and the pulse energies at each stage of amplification, the pulse energies were well below the saturation energies in the first and second amplifier stages. This means we are justified in treating the system as a single amplifier for the purpose of analyzing the pulse shaping.

When the calculated input pulses were fed into the system, they produced the square pulses shown in Fig. 3(b). The black lines show the target (square) pulse shape and the red curves show output pulses of varying duration produced by active shaping of the seed pulse. The obtained pulses match the target pulse, with deviations in amplitude from the target not exceeding 10% over the duration of the pulse. Simulated annealing using the actual output of the amplifier yielded no detectable further improvement in pulse shape.

Since both methods produced virtually identical inputs we can state that for square target pulses, the direct calculation method produces results indistinguishable from the iterative process, giving great confidence in this simplified approach.

Figure 4 compares shaping results (for a 1 μs duration pulse) obtained using the iterative optimization method but in one case (red), shaping the input pulse using direct modulation of the seed diode current, as in [12,13] and in the other case (blue), using gating with the EOM to create shaped pulses. It can be seen that there is a large transient on the pulse in the directly modulated case. This was observed on all pulses produced by direct modulation of the diode. We attribute this to changes in the seed spectrum that arise during pulse build up, as described above. Because the gain is wavelength dependent, changing the centre wavelength and bandwidth during the pulse as it develops will change the gain experienced. The pulse shaping methods used, which do not account for such changes, will not correct for this feature. As expected, this only affects the first few 10s of nanoseconds of the pulse. Using the EOM to shorten and shape the pulses completely removes the issue of diode startup dynamics. It should be noted that this problem could potentially also be addressed in other ways. For example, a diode with an external grating packaged very close to the diode (as are becoming commercially available) might eliminate this problem. It might also be addressed by a more complex iterative approach, with separate fitting of the initial dynamics, but this would require more computation time, and a faster AWG than we possess [12]

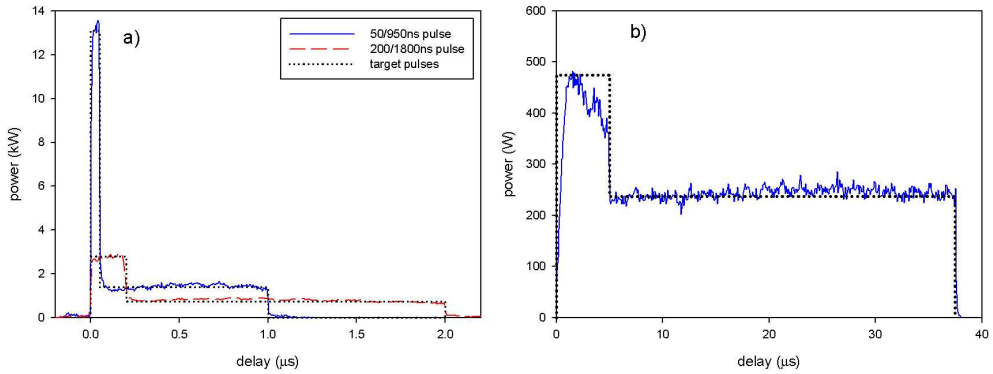

Fig. 5. Two-step pulse shape with (a) low duty cycle, (b) high duty cycle

We also produced various duration two-step pulses at high average power. In order to produce two-step pulses, as shown in Fig. 5, using the iterative method, we simply simultaneously optimized two segments with fixed durations and independent starting heights and exponential factors, so that a total of four parameters required optimization. In simulation, the iterative process converged after ~100 iterations. As observed with the square pulses,

#117239 - $15.00 USD Received 14 Sep 2009; accepted 15 Oct 2009; published 2 Nov 2009

iterations based on the real amplifier output did not improve on the results obtained in simulation.

Figure 5(a) shows results for relatively low duty cycle 2-step pulses, Fig. 5(b) for a high duty cycle pulse. In these experiments the average power was 200 W and the repetition rate 100 kHz, giving a pulse energy of 2 mJ. The duty cycles were 20% and 10% for the two pulses shown in Fig. 5(a). In both cases deviations in amplitude from the target pulse do not exceed 10%. Figure 5(b) shows a pulse generated for an average power of 200 W and a repetition rate of 20 kHz, giving a pulse energy of 10 mJ. The pulse displayed consists of an initial 5 μs section and a final 32.5 μs (75% duty cycle). The final part of the pulse has a power level close to 200W (i.e. near the average power) whilst the power level in the initial section is approximately twice this.

In theory, our approach is not expected to be precisely accurate for high duty cycle pulses, since our analysis ignores pumping during the pulse: there is no replenishment of the inversion during the pulse. This is a reasonable approximation for low duty cycle pulses only. It should be possible to modify the approach described above to allow for repopulation of the upper level by pump absorption during the pulse, but we have not addressed this, as our interest was primarily in short pulses.

However, as we see, this approach is still sufficient to produce fairly good quality pulses even at 75% duty cycle, with a deviation from the target pulse of less than 30% for ~90% of the duration of the first section of the pulse, and considerably better during the second section.

We also generated smooth output pulse shapes. In generating smooth pulses, the advantages of the direct calculation method over the iterative method become clear. In order to produce smooth pulses shapes, such as Gaussian or parabolic pulses by the simulated annealing method, we used input pulses composed of a number of segments. In order to keep the number of independent parameters being optimized at a manageable number, we used straight line segments of fixed duration, with only the initial height of each segment being varied (i.e. only one parameter per segment).

To get convergence on the target pulse using SA with calculated results and using a pulse composed of 12 segments, typically required of order 1000 iterations. With each experimental iteration requiring of order 2 seconds (determined by the CPU time and the time taken to update the waveform on the computer controlled AWG), it was impractical to employ experimental optimization to further improve the results obtained in simulation, negating the most obvious possible advantage of the SA method; i.e. that it does not necessarily depend on our assumptions about ideal amplifier performance but more on the actual performance of the amplifier chain.

It was also observed that with these pulse shapes, on occasion the solution would get stuck at a local minimum which did not correspond very closely to the desired pulse. Although these could be improved upon by varying the annealing parameters, this further indicated the inconvenience of this method for smooth pulse shapes. In contrast, the direct calculation approach requires no choices to be made about fitting parameters, and requires no more processing time for these pulse shapes than for square pulses.

Figure 6 shows results for a targeted parabolic pulse of 1 mJ pulse energy. Figure 7(a) shows various input pulse shapes used and Fig. 7(b) shows the corresponding output pulses. It can be seen that a parabolic input pulse (long dashes) yields an output pulse which is heavily skewed, as expected. Furthermore, the direct calculation method (solid line) in this case produces a significantly better approximation of the targeted pulse shape (dots) than the iterative method (short dashes), which appeared to get stuck at a local minimum. The output pulse produced by the calculation method differed from the target pulse by less than 10% of the peak power over the full duration of the pulse.

#117239 - $15.00 USD Received 14 Sep 2009; accepted 15 Oct 2009; published 2 Nov 2009

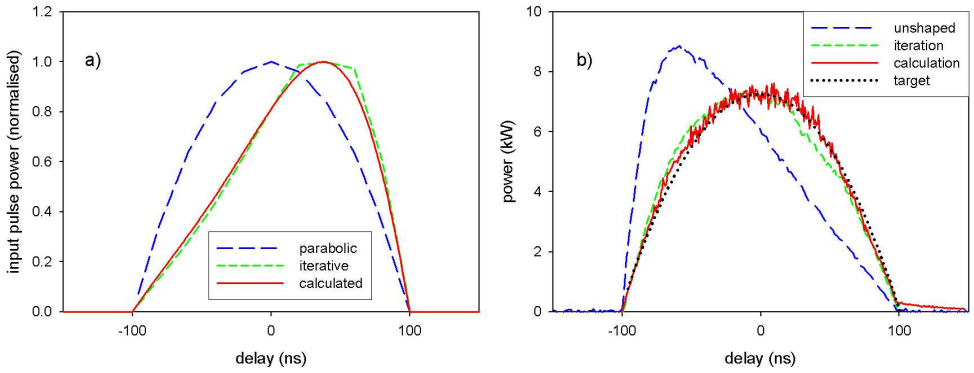

Fig. 6. (a) Input pulses and (b) output pulses obtained by various methods with a targeted parabolic pulse shape

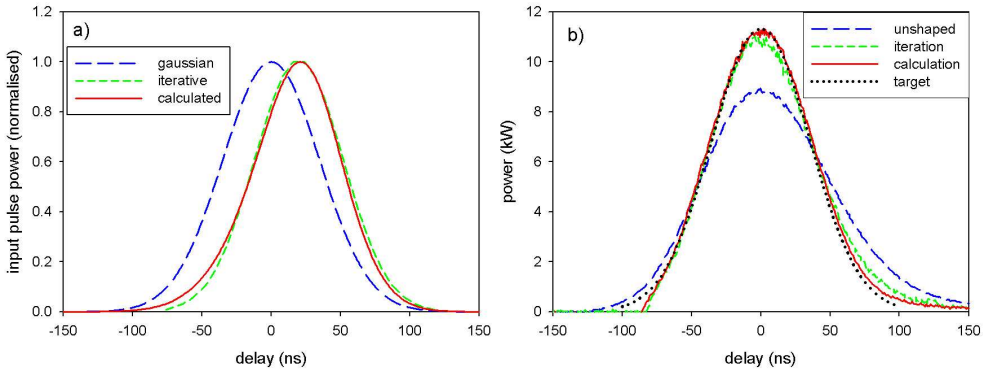

Fig. 7. (a) Input pulses and (b) output pulses obtained by various methods with a targeted Gaussian pulse shape

Figure 7 shows similar outputs for a targeted Gaussian output pulse of 100 ns duration. Again, the pulse energy is 1 mJ. The targeted pulse shape is shown (dotted). The output pulse obtained for an input Gaussian pulse of the desired output duration is shown by long dashes. It can be seen that the effects of gain reshaping are more subtle than in the case of a square pulse; the pulse increases in duration and becomes slightly asymmetric during amplification. The solid curve shows the output pulse obtained using direct calculation. The best result obtained by SA using calculated results is shown by the short dashes. It can be seen, that while both methods produce a result close to the desired pulse shape, direct calculation produced slightly superior results. The deviation from target pulse amplitude is less than 2% of the peak power everywhere within the 10 dB full width of the pulse.

7. Conclusion

We have produced square pulses of up to ~2 mJ energy with a range of durations from ~100 ns upwards in a seeded cascade of Yb-doped fiber amplifiers. We have also produced 2-step pulses and pulses with smooth profiles. We have worked at duty cycles from 1% to 75%. Compared to our previous paper on pulse shaping, we have scaled average power from 10W to 300W by adding a third amplifier.

By using an EOM to shape our seed pulses rather than rely on direct modulation of the seed diode, we have improved the quality of the pulses, avoiding any transients introduced by the operation of the diode or its drive electronics and limitations imposed by its available

#117239 - $15.00 USD Received 14 Sep 2009; accepted 15 Oct 2009; published 2 Nov 2009

dynamic range. This will also allow us to shape a much wider variety of seed lasers, including those which do not have a short pulse operation mode.

The method of calculating the required input pulse from the measured gain parameters of the amplifiers is rapid and allows optimization of smooth pulse shapes, where the iterative method based on pulses composed of simple segments becomes unmanageable due to the number of parameters which need to be optimized. The direct calculation method is shown to produce output pulses which match the target pulse shape at least as well, if not better, than the iterative method for all the pulse shapes examined.

Our method is indifferent to the detailed architecture of the amplifier chain; the only parameters required can be obtained via a single experimental measurement. This will allow the approach to be adapted rapidly to a wide variety of amplifier chains. This should be of significant value in enhancing the use of fiber based MOPA systems for a range of industrial and scientific applications.

#117239 - $15.00 USD Received 14 Sep 2009; accepted 15 Oct 2009; published 2 Nov 2009